NASA

Technical Memorandum 83812

Satellite-Derived Ice Data Sets No. 1: Antarctic Monthly Average Microwave Brightness Temperatures and Sea Ice Concentrations 1973-1976

H. J. Zwally, J. C. Comiso

and C. L. Parkinson

NOVEMBER 1981

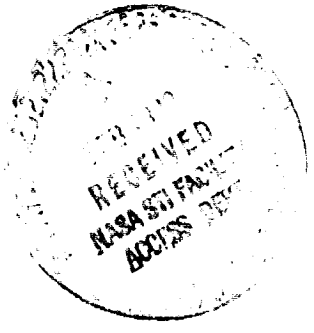

National Aeronautics and
Space Administration

Goddard Space Flight Center
Greenbelt, Maryland 20771

SATELLITE-DERIVED ICE DATA SETS NO. 1: ANTARCTIC MONTHLY AVERAGE MICROWAVE BRIGHTNESS TEMPERATURES AND SEA-ICE CONCENTRATIONS, 1973-1976

H. J. Zwally, J. C. Comiso, and C. L. Parkinson
Goddard Laboratory for Atmospheric Sciences

November 1981

NASA/GODDARD SPACE FLIGHT CENTER
Greenbelt, Maryland 20771

SATELLITE-DERIVED ICE DATA SETS NO. 1: ANTARCTIC MONTHLY AVERAGE MICROWAVE BRIGHTNESS TEMPERATURES AND SEA-ICE CONCENTRATIONS, 1973-1976

H. J. Zwally, J. C. Comiso, and C. L. Parkinson
Goddard Laboratory for Atmospheric Sciences

ABSTRACT

A summary data set concerning 4 years of Antarctic sea-ice conditions has been created and is available on magnetic tape[1]. The data were derived from electrically scanning microwave radiometer (ESMR) brightness temperatures and were mapped into a polar stereographic grid enclosing the 50°S latitude circle. The grid size varies from about 32 by 32 km^2 at the poles to about 28 by 28 km^2 at 50°S. The microwave brightness temperatures of Antarctic sea ice are predominantly characteristic of first-year ice with an emissivity of 0.92 at 19 GHz frequency. Sea ice concentrations were calculated from the brightness temperature data for each grid element with an algorithm that uses an emissivity value of 0.92 and an ice physical temperature estimate from climatological surface air temperatures. Monthly, multiyear monthly, and yearly maps of brightness temperatures and sea ice concentrations were created for the 4 years, except for 7 months for which useable data were insufficient.

1 The data are being released prior to the publication of a detailed analysis in an atlas entitled "Antarctic Sea Ice 1973-1976 from Satellite Passive Microwave Observations" by H. J. Zwally, J. C. Comiso, C. L. Parkinson, W. J. Campbell, F. D. Carsey, and P. Gloersen. Further analysis and application of the data are encouraged and any publication resulting from such study should reference the atlas as well as this document.

SATELLITE-DERIVED ICE DATA SETS NO. 1: ANTARCTIC MONTHLY AVERAGE MICROWAVE BRIGHTNESS TEMPERATURES AND SEA-ICE CONCENTRATIONS, 1973-1976

H. J. Zwally, J. C. Comiso, and C. L. Parkinson
Goddard Laboratory for Atmospheric Sciences
NASA/Goddard Space Flight Center
Greenbelt, Maryland

INTRODUCTION

This report describes a summary data set concerning 4 years of Antarctic sea ice conditions, available on magnetic tape. The data set provides the most extensive available synoptic coverage of Antarctic sea ice, coverage made possible by the 19-GHz ESMR on board the Nimbus 5 satellite launched in December 1972. A detailed description of both the satellite and the instrument can be found in the Nimbus 5 User's Guide (Sabatini, 1972). The unique day/night capabilities of such radiometers and the strong contrast between the brightness temperature, T_B, of the ice and that of water at the 19-GHz frequency make the ESMR instrument suitable for observing spatial and temporal variations of sea-ice cover. The same data will appear in an Antarctic sea-ice atlas (Zwally et al., in preparation) in various forms, including false-color images of T_B at 5 K intervals, ice concentration at 4-percent intervals, and monthly differences in ice concentration at 5-percent intervals. In addition, the ice concentration maps will be presented at larger intervals as black-and-white images and as contour maps. The latter, which show ice concentration contours for 15-, 50-, and 85-percent ice concentration values, are included in this document as well.

The value of such sea-ice data sets for climate studies and for surface energy balance calculations has been cited by Fletcher (1968), Weller (1980), and Ackley (1981). In addition, Zwally and Gloersen (1977) have

noted other scientific applications. The commercial applicability of these data is also well recognized, particularly in areas in which oil exploration is actively pursued. Because of limited resolution (about 30 by 30 km^2), however, the data are more useful for global or large-scale studies than for small-scale studies.

DATA PROCESSING, MAPPING, AND COMPILATION

The primary source of orbital Earth-located and calibrated radiometer data is the set of calibrated brightness temperature (CBT) tapes. The CBT tapes contain the time, calibration parameters, measured brightness temperatures, and corresponding geographical coordinates (Wilheit, 1972). The tapes are structured so that, when written at 6250 bits per inch, each tape contains about 180 orbits of data stored in separate files. Table 1 lists the format of each file in the CBT tape. These tapes were written in binary format and were blocked so that each block contains 50 records with 560 bytes per record.

To provide synoptic representation of the data in the polar regions for both spatial and temporal studies, the orbital data were projected to polar stereographic maps and accumulated at fixed time intervals. A polar stereographic map is a projection of points on the Earth's surface onto a plane tangent to the surface at a pole (north or south) with the vertex of the projection being the opposite pole. Figure 1 illustrates the concept, with a point (B) on the Earth's surface being projected to the polar plane at C through a line from the vertex pole (A) to B. The grid size for these maps is 293 by 293, with each map cell representing an area ranging from about 32 by 32 km^2 near the poles to about 28 by 28 km^2 near 50° latitude. The geographical coordinates of the center of the radiometer

field-of-view determine the cell into which the data is placed. Overlapping data in a cell from successive orbits are averaged to give a single brightness temperature average taken to be located at the center of the cell.

The coordinates of each point in the projected map are determined as follows. The distance (r) from the Pole to the projected point is calculated from:

$$r = d \tan \alpha \tag{1}$$

where d is the diameter of the Earth, and α is the angular projection at the opposite pole expressed in terms of the latitude ϕ as follows:

$$\alpha = \frac{90 - \phi}{2} . \tag{2}$$

With λ the east longitude and the Greenwich meridian coinciding with the positive ordinate of the map, the x and y components of the data element using Figure 1 are given by:

$$x = d \tan \alpha \cos (90^\circ - \lambda) \tag{3}$$

$$y = d \tan \alpha \sin (90^\circ - \lambda) \tag{4}$$

The standard 293 by 293-grid maps are constructed from the foregoing coordinate system by defining the location of each map cell by the following set of coordinates (I,J):

$$I = 147 + x + 0.5 \tag{5}$$

$$J = 147 - y + 0.5 \tag{6}$$

The value of 0.5 included in equations 5 and 6 properly positions the map cell at the center of its geographic location.

Full coverage of the entire polar area could be obtained from a sequence of six satellite orbits or one-half day of good data if the full set of 78 beam positions is used. However, because of the large disparity in

the radiometer field of view from the outer beam position to the middle beam position (i.e., 70 by 140 km^2 compared to 25 by 25 km^2), only the middle 52 beam positions were used equatorward of 85 degrees latitude. This method provides a swath-angle coverage of $\pm 30.5°$, corresponding to a spatial coverage of about 1280 km on the Earth's surface, and a minimum resolution of 29 by 42 km^2. Because the area poleward of 85° latitude is observed by the outer beam positions only, the outer positions were used to cover this region. With this restriction on beam positions and with additional rejection of data because of instrumental problems, approximately 3 days of data are usually required for providing adequate spatial coverage of the polar regions. Three-day average maps were therefore generated for all periods, from launch until May 1977, that contained valid data.

Each data element on the polar stereographic maps represents a quantity (e.g., brightness temperature) averaged over the number of measurements made in that area within the specified time period. For a 3-day average map, this number of measurements, called population, ranges from 0 to 35, depending on the location of the data element and the availability of good data. During the analysis of the data, this value was used to determine how representative the data-point measurement is as an average over the given time. For most of the polar maps, a record of population normally follows a data record.

Because of data loss caused by processing and calibration problems, as many as 20 percent of the data cells were empty on some 3-day average maps. The 20 percent data loss occurred much more frequently after Nimbus 6 was launched in 1976, when Nimbus 5 data became available only

every other day. Fortunately, most of these empty cells are located outside the range of the seasonal sea-ice extent. For completeness and proper weighting of data in the monthly average maps, some interpolations were made to fill in the empty cells in the 3-day average maps. A combination of temporal and spatial interpolation was employed. Normally, maps with very few empty cells were filled by linear spatial interpolation. For gaps involving four or more cells, however, time interpolation gave a more consistently satisfactory result. To fill in an empty cell by time interpolation, the average was taken of the brightness temperature in the cell for the previous 3-day average map and the one immediately after. In the rare cases when necessary, the procedure was extended to use data for up to three 3-day averages before and after the empty cell.

The brightness temperature of the ocean is expected to have minimal or no seasonal dependence, because the emissivity is inversely proportional to the surface physical temperature (Wilheit, 1972). Although brightness temperature is affected by roughness, foam cover, water vapor, and rainful, none of these have seasonal characteristics. However, studies of the temporal variation of T_B in the southern ocean revealed some unexpected shifts; the conclusion was that these could be caused only by calibration or instrumental problems. Appropriate adjustments in T_B were made as follows.

To investigate the time dependence of T_B, the data for each pixel in the monthly maps between 55° and 65°S were binned and plotted. The contribution from the ocean appeared as a narrow peak with an average width of about $\pm$ 4 K. Figure 2 shows the brightness temperatures of these peaks for

each month of available ESMR data. In 1973, the values dropped by approximately 8 K from January to July, and, in 1976, a much sharper dip occurred in May, followed by a recovery in July and a general decrease for the remainder of the year. During 1974 and 1975, T_B was nearly constant with time. The apparently anomalous shift in T_B in 1976 was further studied by examining both ocean and highly concentrated sea-ice areas and using 3-day average maps. The shifts in brightness temperature in both ocean and ice areas occurred at about the same time. Furthermore, although the initial downward shift is about 10 K for the ocean and 8 K for sea ice, the recovery shift is about 18 K for the ocean and 25 K for sea ice. The latter shift would require a change in physical temperature of about 27 K on the ice and 40 K in the water, assuming emissivity to be constant during the time period. Because of the abrupt nature of the shifts and their magnitude, it is not possible to attribute them to physical effects in the ocean or the atmosphere.

Examination of the time variation of T_B of the Antarctic ice sheets also indicated that the smaller dip observed in 1973 resulted from calibration problems. The short-term year-to-year variation of T_B in the ice sheets was expected to be minimal because the seasonal physical temperature--the most significant variable expected to cause such a variation--did not change much during the 4-year period. By adjusting to force the ocean temperatures to remain constant, the T_B in the ice sheets also became more consistent during the 4 years. Comiso and Zwally (1980) discuss the procedures used for normalizing the data in response to these anomalous shifts.

EXTRACTION OF SEA-ICE CONCENTRATION FROM ESMR

Within the ice pack, the brightness temperature of a pixel area derives from various sources--the water and ice within the field of view, and the atmosphere. To a good approximation,

$$T_B = C_W \varepsilon_W T_W + C_I \varepsilon_I T_I + T_A \tag{7}$$

where ε_W, T_W, and C_W are emissivity, surface physical temperature, and areal percentage of water, and ε_I, T_I, and C_I are the corresponding values for sea ice. T_A is the contribution attributable to the atmosphere and includes the direct upwelling radiation, the downwelling radiation reflected from the surface, and the radiation from space reflected by the surface. Because the reflectance of water is different from that of ice, the atmospheric contribution can be separated into contributions over water, T_{AW}, and over ice, T_{AI} (i.e., $T_A = C_W T_{AW} + C_I T_{AI}$). The atmospheric opacity in the polar region has been estimated to be very small and was neglected. Also, $C_W + C_I = 1$ and ε_I was determined empirically to be about 0.92.

The ice concentration, C_I, can thus be determined from equation 7:

$$C_I = \frac{T_B - T_O}{\varepsilon_I T_{eff} - T_O} \tag{8}$$

where $T_O = \varepsilon_W T_W + T_{AW}$ is the measured brightness temperature of the water determined from the data, and $T_{eff} = T_I + T_{AI}/\varepsilon_I$ is the effective surface physical temperature. The value of T_{AW} was calculated by using radiative transfer modeling of the atmosphere (Nieman and Wilheit, private communication) and was estimated over the ocean to be about 8 K. The value of T_{AI} is considerably smaller because the reflectivity of ice is substantially lower than that of water, and the contribution of down-welling

radiation reflected from the surface is therefore smaller. In the polar regions, the atmospheric contribution to the brightness temperature is minimal because the humidity and the water-vapor content in the atmosphere is very low. Therefore, T_{eff} is taken to be equal to T_I. The appropriate physical temperature, T_I, is the temperature at the top of the sea ice below the snow cover, because most of the observed radiation emanates from a thin top layer of saline ice. In the absence of real-time physical temperature data, T_I was estimated from a compilation of climatological surface air temperatures (Jenne et al., 1974) as follows. The actual temperature of the top sea-ice surface lies between the surface air temperature, T_{air}, interpolated from the climatological data, and the temperature of the water underneath the ice. It can be expressed by:

$$T_I = T_{air} + f(T_m - T_{air}) \tag{9}$$

where T_m is the melting temperature of ice, and f is an empirical parameter deduced from the ESMR data. Figure 3 shows a histogram of the ice-covered area in the Weddell Sea in July 1973 as a function of ice concentration. The parameter f was adjusted until the backward peak of the histogram fell off approximately near the 100-percent region, allowing for several degrees of uncertainty in the observed brightness temperatures. The value of $f = 0.25$ obtained by this procedure gives temperatures of the snow/ice interface relative to T_{air}, which are in good agreement with surface measurements on first-year ice in the Arctic (Ramseier, private communication). The value of f will vary spatially with the thicknesses of the ice and the snow cover, but $f = 0.25$ appears to be a good average value. Also, analysis of the open-ocean area in the vicinity of the ice pack showed that $T_o = 135$ K. Thus, two reference points were used in determining ice concentration.

DATA STORAGE AND RETRIEVAL

The 4-year data sets of southern ocean ESMR brightness temperatures, plus the sea ice concentrations calculated with the foregoing equations and considerations, are stored in sequential arrays on magnetic tape. Each polar-map cell is associated with a matrix element, D(J,I), that represents the average value of the data over the number of measurements represented by the population matrix, P(J,I), where J and I are as defined in equations 6 and 7. The sequence in which the data are stored is shown in Table 2. A 20-word, 4 byte-per-word header preceding each map describes the type of map, the size of the grid, the scaling, the time interval the map data were accumulated, and other information associated with the data (Table 3). This header is followed by a sequence of 293 times 2 data and population records, each 293 words long representing D(J,I) and P(J,I) for constant I and for J varying from 1 to 293. For the data and population records, each word is 2 bytes, making each record 586 bytes. Although only the first 80 bytes are meaningful on the header record, this record also has a length of 586 bytes. The data are blocked when written on tape so that there are 8 records per block.

All the monthly data have been placed on one magnetic tape written at 6250 bits per inch. The 41 monthly T_B's from 1973 to 1976 are stored in files 1 through 41 in chronological order, followed by 12 multiyear monthly T_B's and 5 yearly and 4-year average T_B maps. These are followed by the corresponding 58 ice-concentration maps, the 12 climatological surface air temperatures, and the 12 climatological pressure maps. Table 4 summarizes the population and overall quality of each polar map. Figures 4 to 13 show contour maps of monthly and multiyear monthly ice concentrations. Three values of ice concentration were contoured: 15, 50, and 85 percent.

A detailed analysis of the data set and descriptions of the ice conditions are given in the aforementioned atlas (Zwally et al., in preparation) which includes pseudo color images of brightness temperature, sea ice concentration, changes in ice concentration, and multiyear average concentrations. Also included are graphs of the area of ice in various concentration categories as a function of time for the entire southern ocean and in five geographical sectors. The amount of open water, mean ice concentration, and actual ice areas are shown. The atlas further includes discussions of the observed interannual variations and the characteristics of the growth-decay cycle.

ACKNOWLEDGEMENTS

The authors wish to thank M. Osborne, R. Pelletier, and D. Love from Computer Sciences Corporation, and J. Manning and D. Johnson from Computer Sciences Technicolor Associates for programming and technical support in the preparation of the data sets. We also appreciate discussions on these data sets with Drs. P. Gloersen, W. J. Campbell, F. D. Carsey and R. Ramseier.

REFERENCES

Ackley S. F., "A Review of Sea-ice Weather Relationships in the Southern Hemisphere," Sea Level, Ice and Climatic Change (Proceedings of the Canberra Symposium, December 1979). IAHS Publication 131, 1981.

Comiso, J. C., and H. J. Zwally, "Corrections for Anomalous Time Dependent Shifts in the Brightness Temperature from the Nimbus 5 ESMR," NASA TM-82055, 1980.

Fletcher, J. O., 1968: The influence of the Arctic pack ice on climate. In: Meteorological Monographs, J. M. Mitchell, Jr., ed., (Am. Met. Society), 8, 93-99.

Jenne, R. L., H. L. Crutcher, H. Van Loon, and J. J. Taljaard, "A Selected Climatology of the Southern Hemisphere: Computer Methods and Data Availability," NCAR-TN/STR-92, 1974.

Sabatini, R. R., ed., Nimbus 5 User's Guide, NASA/Goddard Space Flight Center, 1972.

Weller, G., "Spatial and Temporal Variations in the South Polar Surface Energy Balance," Monthly Weather Review, 108, 1980, pp.2006-2014.

Wilheit, T. T., "The Electrically Scanning Microwave Radiometer (ESMR) Experiment," Nimbus 5 User's Guide, NASA/Goddard Space Flight Center, 1972, pp. 59-105.

Zwally, H. J., J. C. Comiso, C. L. Parkinson, W. J. Campbell, F. D. Carsey, and P. Gloersen, "Antarctic Sea Ice Cover 1973-1976 from Satellite Passive Microwave Observations," NASA SP, in preparation.

Zwally, H. J., and P. Gloersen, "Passive Microwave Images of the Polar Regions and Research Applications," Polar Rec., 18, 1977, pp.431-450.

Table 1
CBT Data Record Format for ESMR

Word	Quantity	Units	Scale	Description
1	Year	Year		Year associated with data
2	Day	Days		
3	Hour	Hours		
4	Minute	Minutes		
5	Second	Seconds		
6	Program ID			Unique Program Identification
7	Pitch error	Degrees	x10	Pitch fine error
8	Roll error	Degrees	x10	Roll fine error
9	RMP Indicated Rate high		x10	
10	Latitude	Degrees	x10	Latitude of subsatellite point
11	Longitude	Degrees	x10	Longitude of subsatellite point
12	Height	Kilometers		Height of spacecraft
13	Hot-load mean		x10	
14	Hot load		x100	
15	Cold-load mean		x10	
16	Cold load		x100	
17	MUX 1			Average antenna temperature
18	MUX 2			Phase-shift temperature
19	MUX 3			Ferrite-switch temperature
20	MUX 4			Ambient load temperature
21	MUX 5			Hot-load temperature
22	MUX 6			Automatic gain control
23-41	Engineering data			
42	Beam Position 79			
43-46	MUX 1-MUX 4			
47-124	Latitude	Degrees	x10	Latitudes of the 78 scan positions
125-202	Longtitude	Degrees	x10	Longitudes of the 78 scan positions
203-280	Brightness temperature	Kelvins	x10	Brightness temperatures of the 78 scan positions

Source: Nimbus 5 User's Guide, 1972.

Table 2

Standard Format* for Polar Stereographic Maps

Record Number	Length (bytes)	Format	Number of Words	Description
1	586	146A4,A2	147	Heading (only the first 20 words are meaningful
2	586	293A2	293	Row 1 data
3	586	293A2	293	Observation population of row 1
4	586	293A2	293	Row 2 data
5	586	293A2	293	Observation population of row 2
.	.	.	.	.
.	.	.	.	.
.	.	.	.	.
586	586	293A2	293	Row 293 data
587	586	293A2	293	Observation population of row 293

*Data format 2 indicates standard format (see Table 3).

Table 3

Header Record for Polar Stereographic Maps

Word	Type	Number of bytes/words	Description
1	A*4	4	Projection type (1 for polar stereographic)
2	A*4	4	Number of columns (293)
3	A*4	4	Number of rows (293)
4	A*4	4	Scale (2.5×10^6)
5	A*4	4	Latitude enclosed (-50.0°)
6	A*4	4	Greenwich orientation (270°)
7	A*4	4	Radius of the Earth
8	A*4	4	J-coordinate of the pole (147)
9	A*4	4	I-coordinate of the pole (147)
10-11	A*4	4	Data type* (TB, ICE CON, SURF TEMP, or CLIM PRES)
12	A*4	4	Start time (day)
13	A*4	4	Start time (hour)
14	A*4	4	Start time (minutes)
15	A*4	4	Stop time (day)
16	A*4	4	Stop time (hour)
17	A*4	4	Stop time (minutes)
18	A*4	4	Year data was colected
19	A*4	4	Data format (2 for standard format)
20	A*4	4	Data Identification
21-146	A4	4	Meaningless
147	A2	2	Meaningless

* Variable abbreviations for words 10 and 11 are as follows: TB is brightness temperature, ICE CON is ice concentration, SURF TEMP is mean monthly climatological surface air temperature, and CLIM PRES is mean monthly climatological sea level pressure.

Table 4

Nimbus 5 Ice Data Set

Date	Time Interval (Julian Date)	Population	File No.	Data Quality
1. ESMR Brightness Temperature Maps				
January 1973	001-031	238	1	Good
February 1973	032-059	287	2	Good
June 1973	152-181	342	3	Good
July 1973	182-212	271	4	Good
September 1973	249-273	127	5	Fair
October 1973	274-304	270	6	Good
November 1973	305-332	261	7	Good
December 1973	336-265	211	8	Good
January 1974	001-031	263	9	Good
February 1974	032-059	305	10	Good
March 1974	060-081	247	11	Good
April 1974	097-120	260	12	Good
May 1974	121-151	274	13	Good
June 1974	152-181	296	14	Good
July 1974	182-212	222	15	Good
August 1974	213-243	203	16	Good
September 1974	244-273	321	17	Good
October 1974	274-304	256	18	Good
November 1974	305-334	275	19	Good
December 1974	335-364	323	20	Good
January 1975	001-028	333	21	Good
February 1975	032-059	269	22	Good
March 1975	060-088	298	23	Good
April 1975	098-106	69	24	Poor
May 1975	122-151	325	25	Good
September 1975	244-273	62	26	Poor
October 1975	274-304	124	27	Fair
November 1975	305-334	112	28	Fair
December 1975	335-365	157	29	Fair
January 1976	001-031	116	30	Fair
February 1976	032-060	154	31	Fair
March 1976	061-091	146	32	Fair
April 1976	092-121	179	33	Fair
May 1976	122-152	151	34	Fair
June 1976	153-182	148	35	Fair
July 1976	186-213	155	36	Fair
August 1976	214-244	189	37	Fair
September 1976	245-274	163	38	Fair
October 1976	275-305	173	39	Fair
November 1976	306-335	169	40	Fair
December 1976	336-365	104	41	Fair

Table 4

Nimbus 5 Ice Data Sets (continued)

Date	Time Interval (Julian Date)	Total Orbits	File No.	Data Quality
January 1973-76	001-031	993	42	Good
February 1973-76	032-060	1015	43	Good
March 1974-76	061-091	691	44	Good
April 1974-76	092-121	508	45	Fair
May 1974-76	122-152	750	46	Good
June 1973/74/76	153-182	786	47	Good
July 1973/74/76	183-213	648	48	Good
August 1974/76	214-244	392	49	Fair
September 1973-76	245-274	673	50	Good
October 1973-76	275-305	823	51	Good
November 1973-76	306-335	817	52	Good
December 1973-76	336-365	795	53	Good
1973	001-365	2050	54	Fair
1974	001-365	3245	55	Good
1975	001-365	1749	56	Fair
1976	001-366	1847	57	Good
1973-76	001-365	8891	58	Fair
2. Sea Ice Concentration Monthly Maps				
January 1973	001-031	281	59	Good
February 1973	032-059	287	60	Good
June 1973	152-181	342	61	Good
July 1973	182-212	271	62	Good
September 1973	249-273	127	63	Fair
October 1973	274-304	270	64	Good
November 1973	305-332	261	65	Good
December 1973	336-265	211	66	Good
January 1974	001--31	263	67	Good
February 1974	032-059	305	68	Good
March 1974	060-081	247	69	Good
April 1974	097-120	260	70	Good
May 1974	121-151	274	71	Good
June 1974	152-181	296	72	Good
July 1974	182-212	222	73	Good
August 1974	213-243	203	74	Good
September 1974	244-273	321	75	Good
October 1974	274-304	256	76	Good
November 1974	305-334	275	77	Good
December 1974	335-364	322	78	Good
January 1975	001-028	333	79	Good
February 1975	032-059	269	80	Good
March 1975	060-088	298	81	Good
April 1975	098-106	69	82	Poor
May 1975	122-151	325	83	Good
September 1975	244-273	62	84	Poor

Table 4

Nimbus 5 Ice Data Sets (continued)

Date	Time Interval (Julian Date)	Total Orbits	File No.	Data Quality
October 1975	274-304	124	85	Fair
November 1975	305-334	112	86	Fair
December 1975	335-365	157	87	Fair
January 1976	001-031	116	88	Fair
February 1976	032-060	154	89	Fair
March 1976	061-091	146	90	Fair
April 1976	092-121	179	91	Fair
May 1976	122-152	151	92	Fair
June 1976	153-182	148	93	Fair
July 1976	186-213	155	94	Fair
August 1976	214-244	189	95	Fair
September 1976	245-274	163	96	Fair
October 1976	275-305	173	97	Fair
November 1976	306-335	169	98	Fair
December 1976	336-365	104	99	Fair
January 1973-6	001-031	993	100	Good
February 1973-6	032-060	1015	101	Good
March 1974-6	061-091	691	102	Good
April 1974-6	092-121	508	103	Fair
May 1974-6	122-152	750	104	Good
June 1973,74,76	153-182	786	105	Good
July 1973,74,76	183-213	648	106	Good
August 1974,76	214-244	392	107	Fair
September 1973-6	245-274	673	108	Good
October 1973-6	275-305	823	109	Good
November 1973-6	306-335	817	110	Good
December 1973-6	336-365	795	111	Good
1973	001-365	2050	112	Fair
1974	001-365	3245	113	Good
1975	001-365	1749	114	Fair
1976	001-366	1847	115	Good
1973-6	001-365	8891	116	Good
3. Monthly Climatological Surface Temperature Maps				
January	001-031		117	
February	032-059		118	
March	060-081		119	
April	097-120		120	
May	121-151		121	
June	152-181		122	
July	182-212		123	
August	213-243		124	
September	244-273		125	

Table 4

Nimbus 5 Ice Data Sets (continued)

Date	Time Interval (Julian Date)	Total Orbits	File No.	Data Quality
October	274-304		126	
November	305-334		127	
December	335-364		128	
4. Monthly Climatological Sea-Level Pressure Maps				
January	001-031		129	
February	032-059		130	
March	060-081		131	
April	097-120		132	
May	121-151		133	
June	152-181		134	
July	182-212		135	
August	213-243		136	
September	244-273		137	
October	274-304		138	
November	305-334		139	
December	335-364		140	

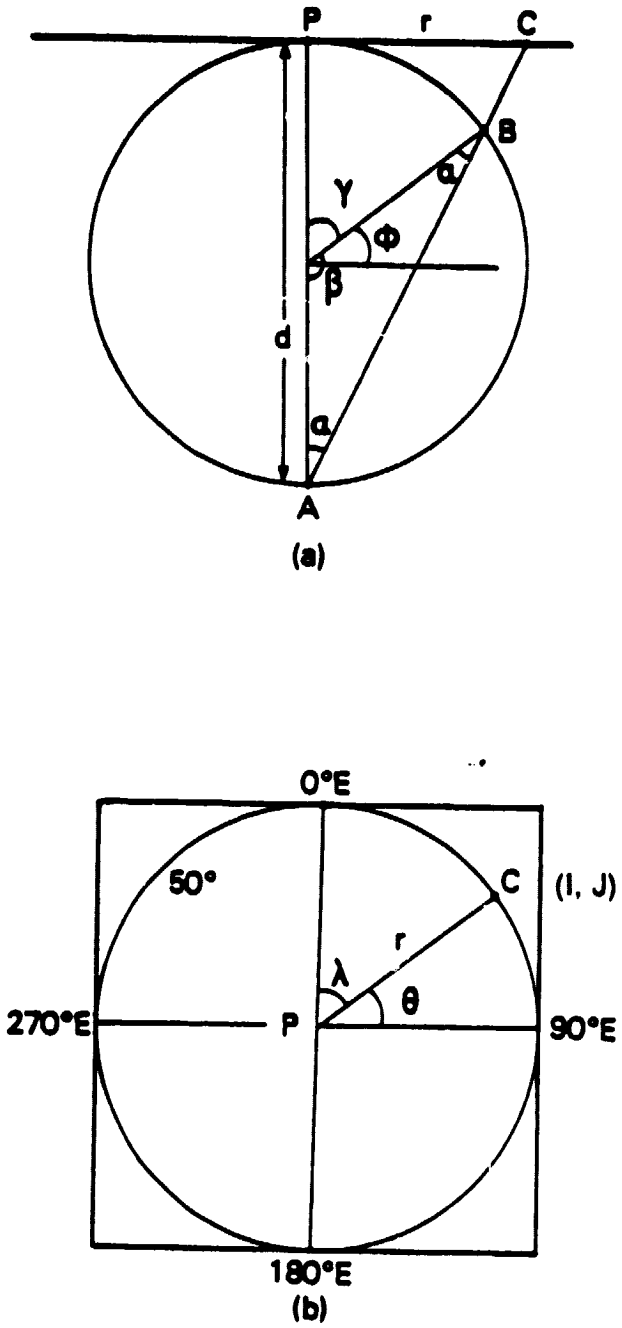

Figure 1. Schematic Diagram for Polar Stereographic Mapping.

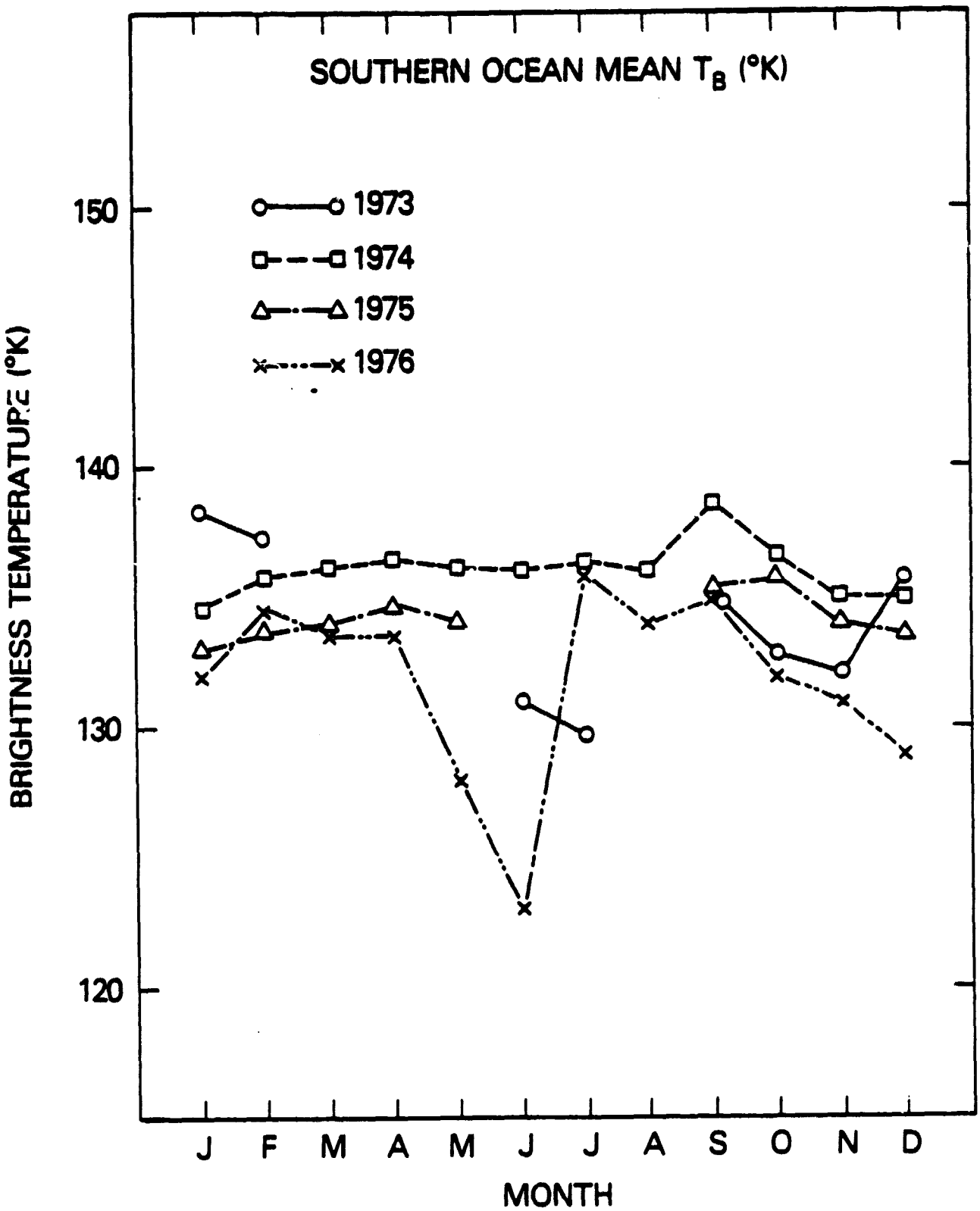

Figure 2. Mean brightness temperatures of the ocean from monthly average maps for 1973-1976 before correction for calibration shifts.

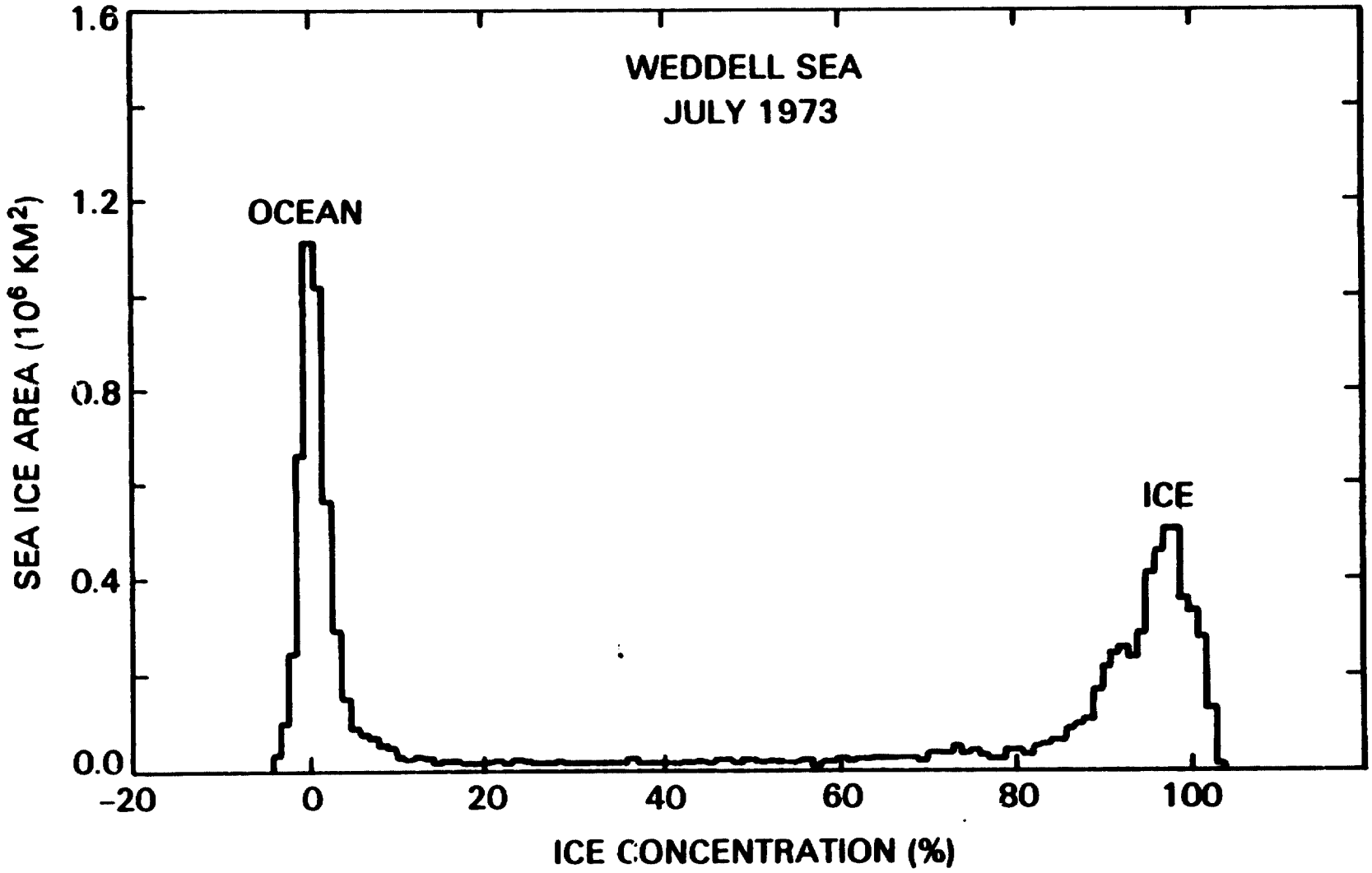

Figure 3. Ice-concentration distribution near the Weddell Sea in July 1973.

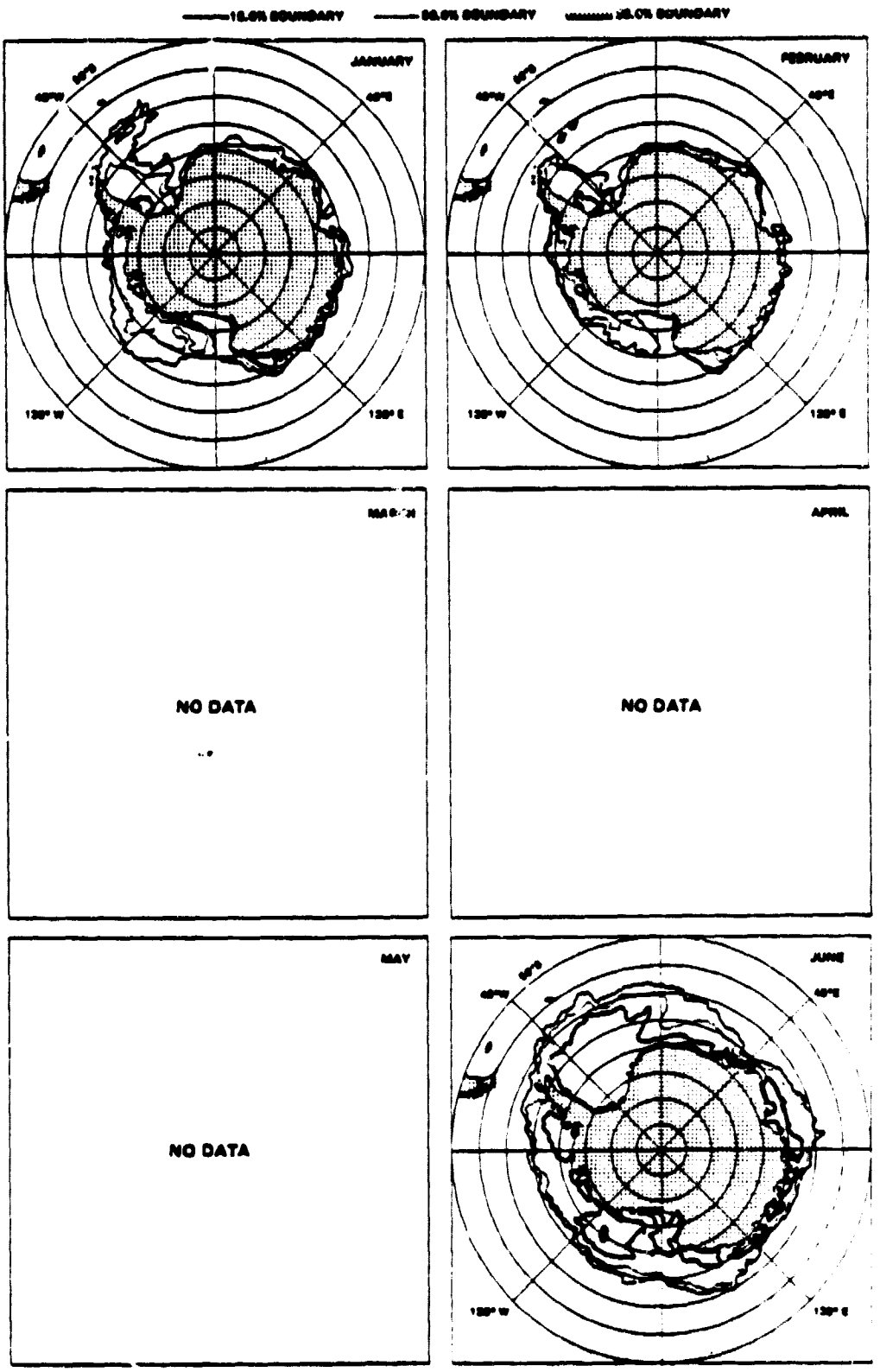

Figure 4. Monthly ice-concentration contours for January through June 1973.

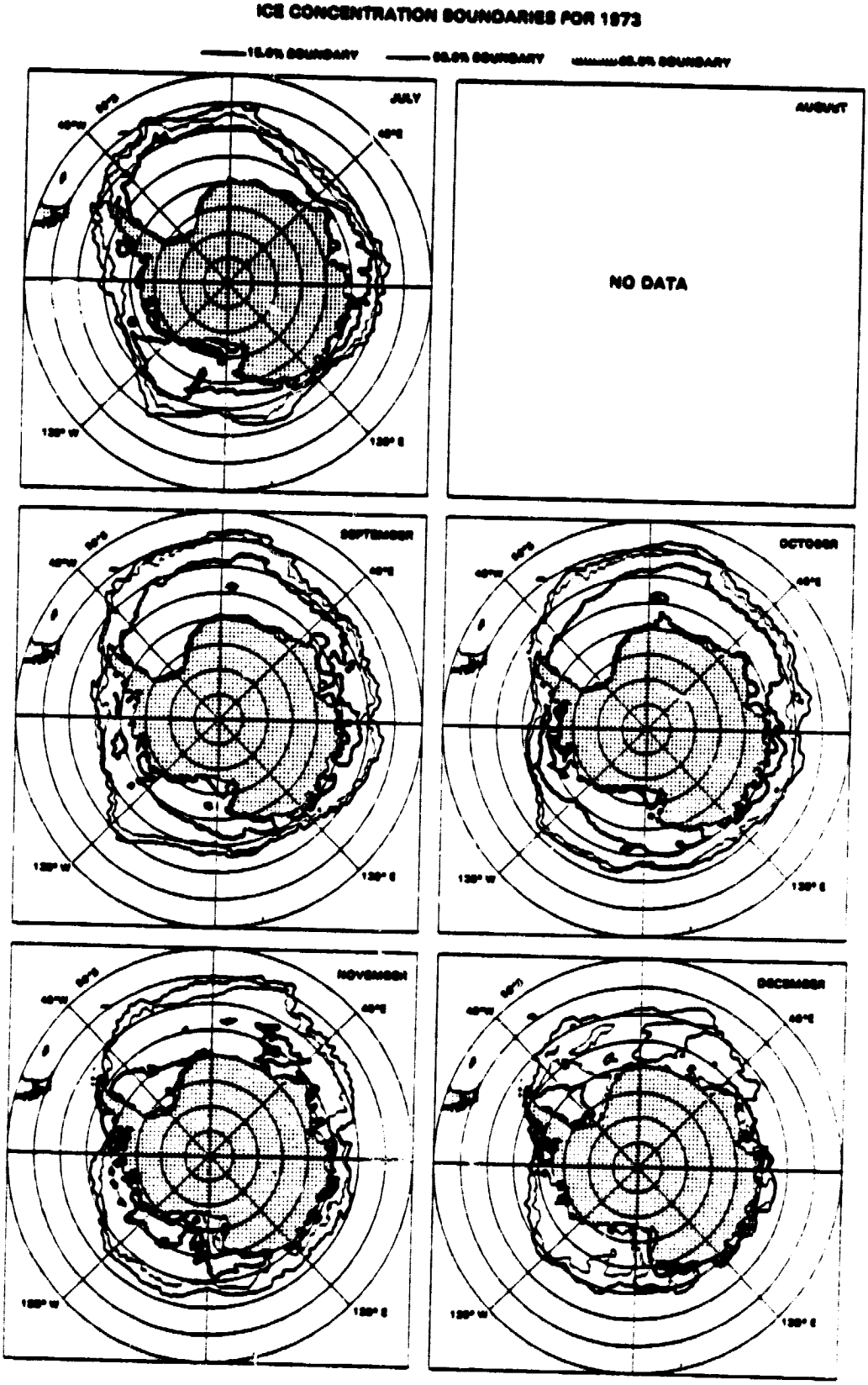

Figure 5. Monthly ice-concentration contours for July through December 1973.

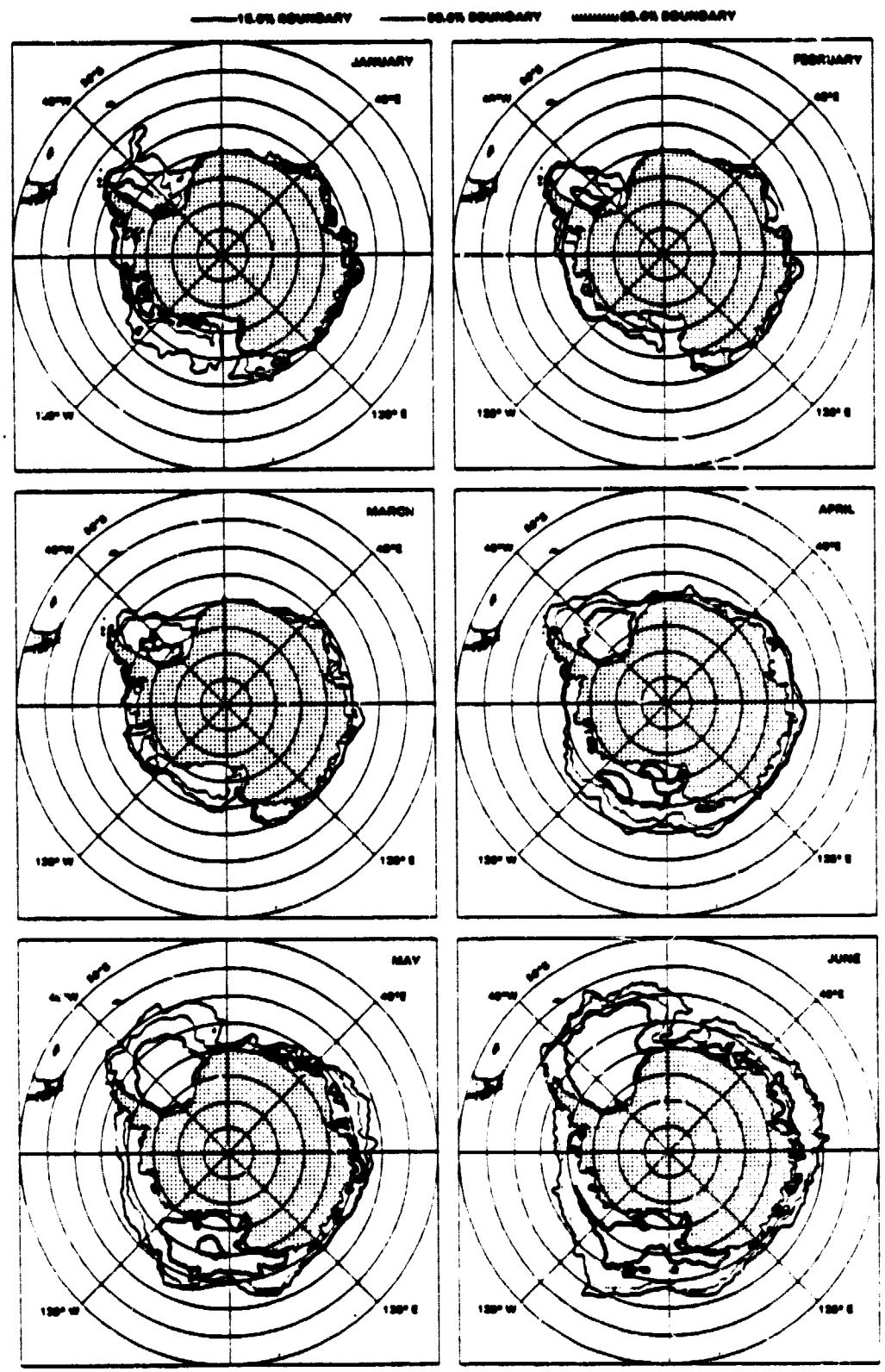

Figure 5. Monthly ice-concentration contours for January through June 1974.

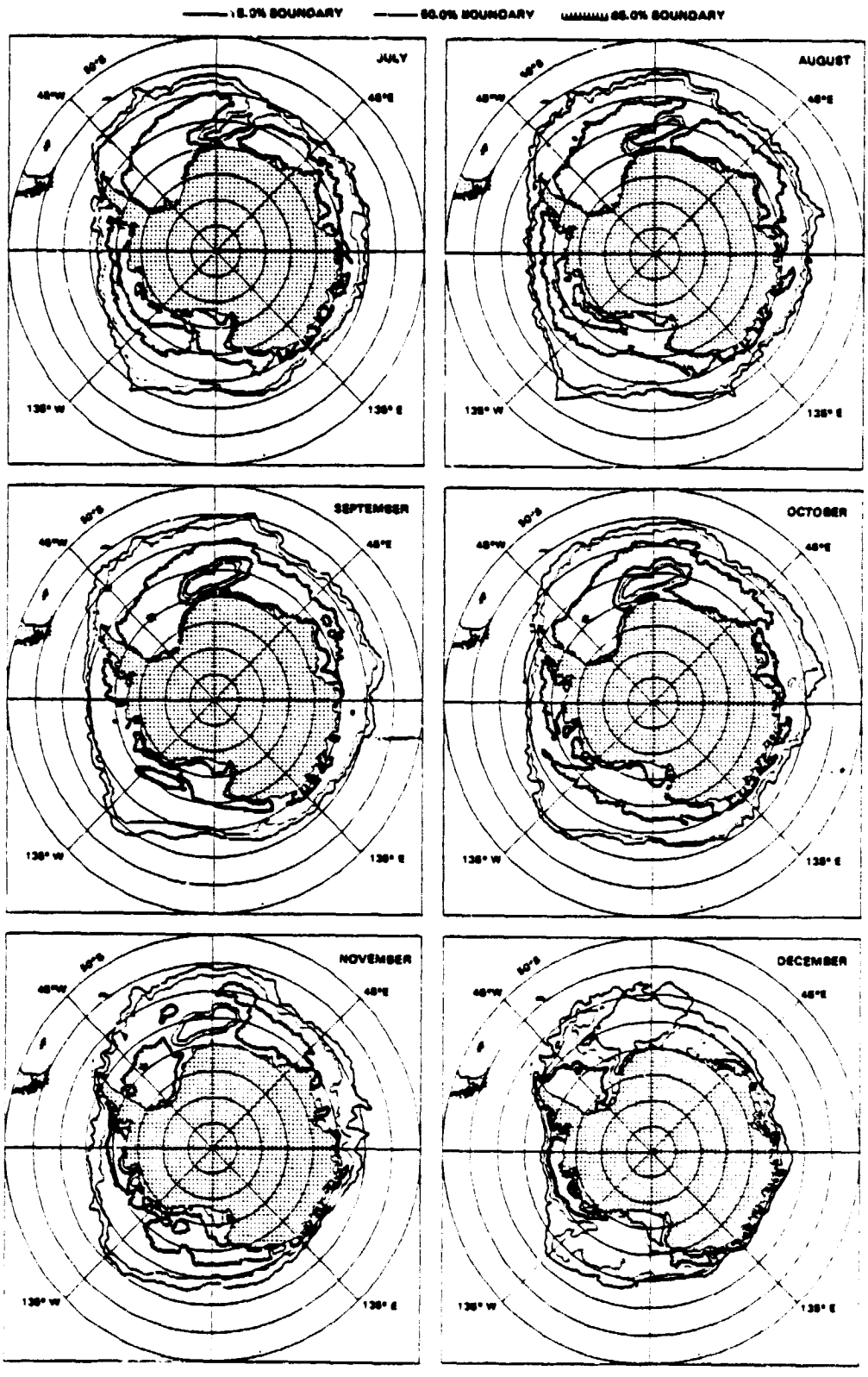

Figure 7. Monthly ice-concentration contours for July through December 1974.

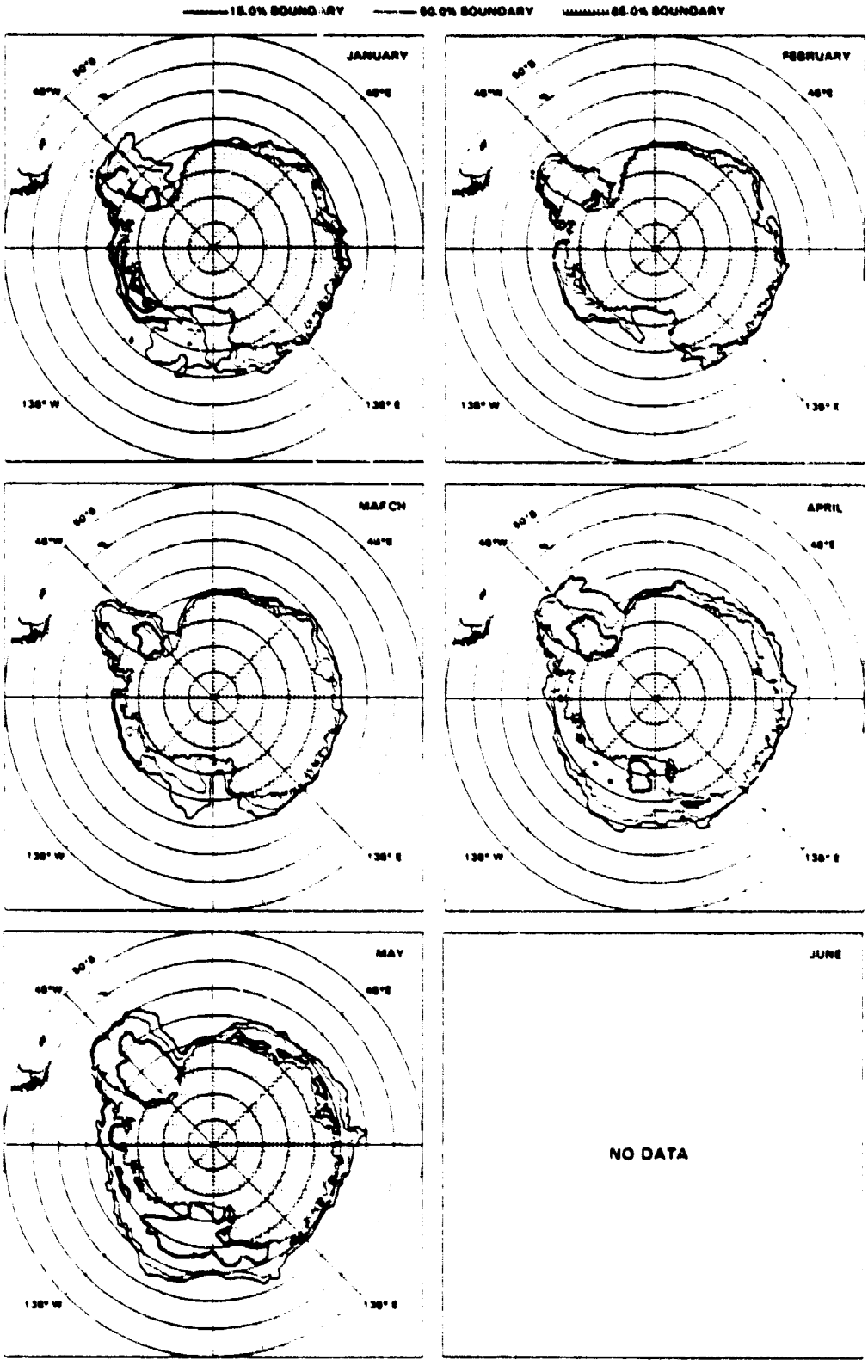

Figure 8. Monthly ice-concentration contours for January through June 1975.

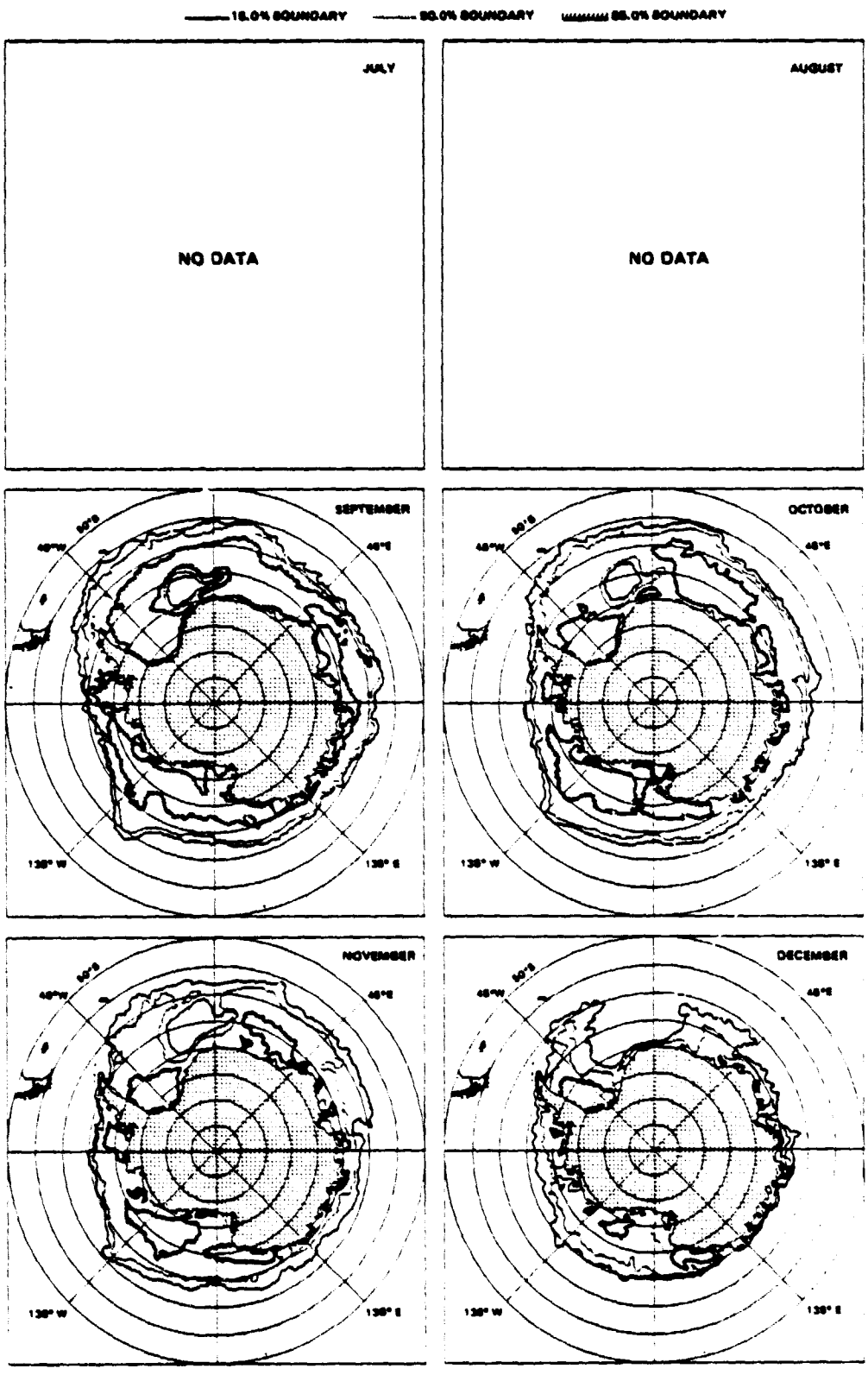

Figure 9. Monthly ice-concentration contours for July through December 1975.

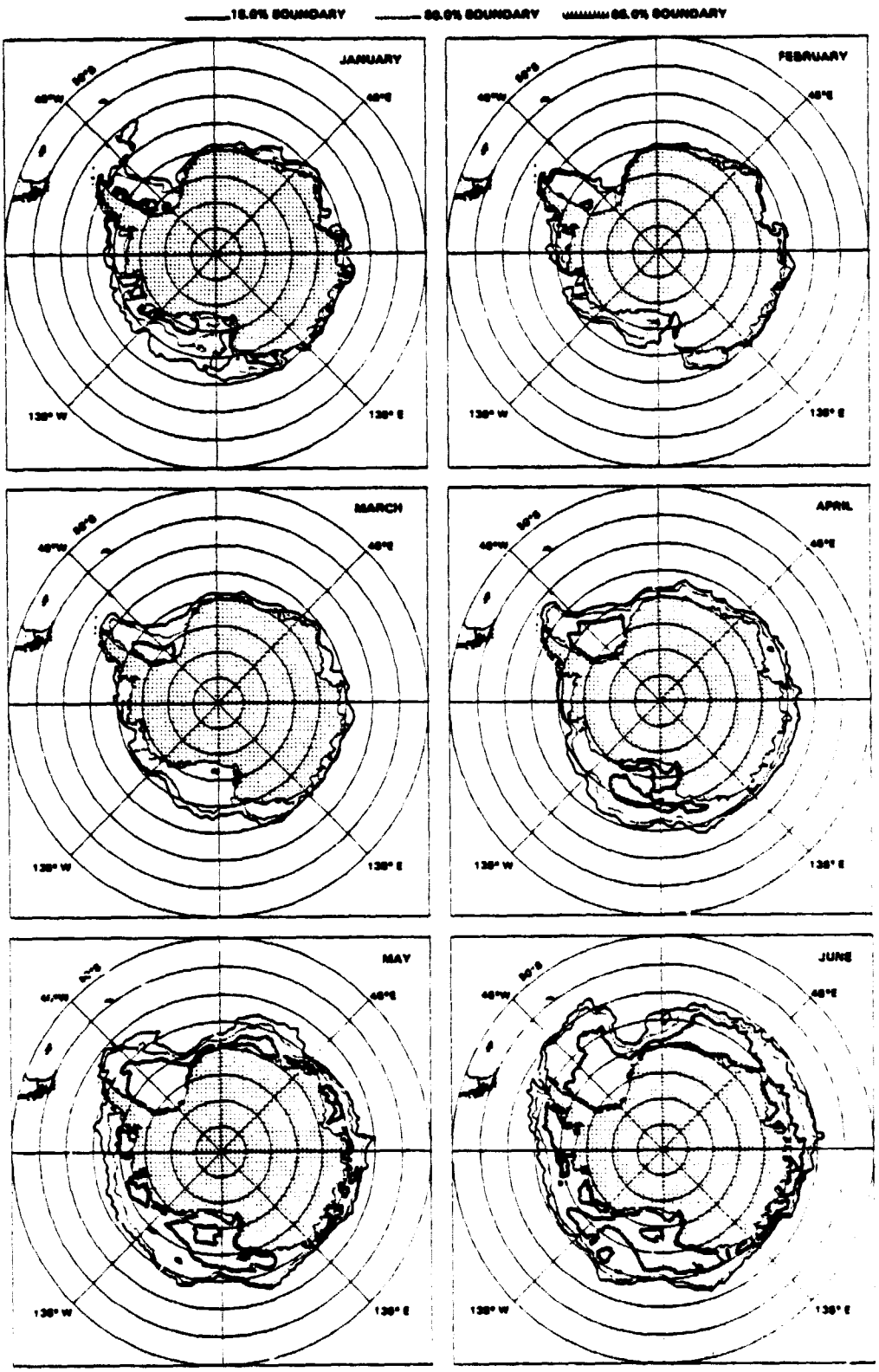

Figure 10. Monthly ice-concentration contours for January through June 1976.

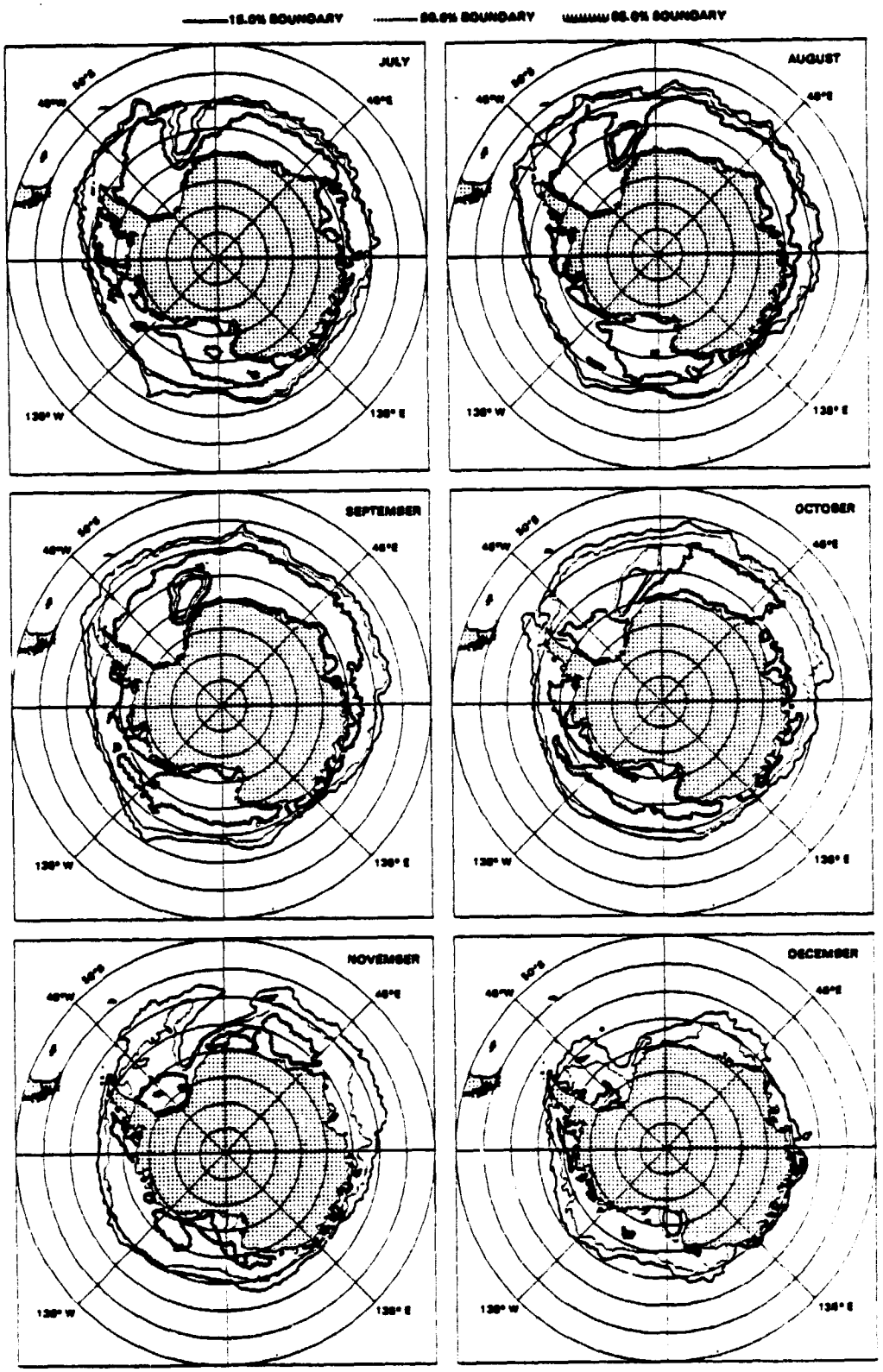

Figure 11. Monthly ice-concentration contours for July through December 1976.

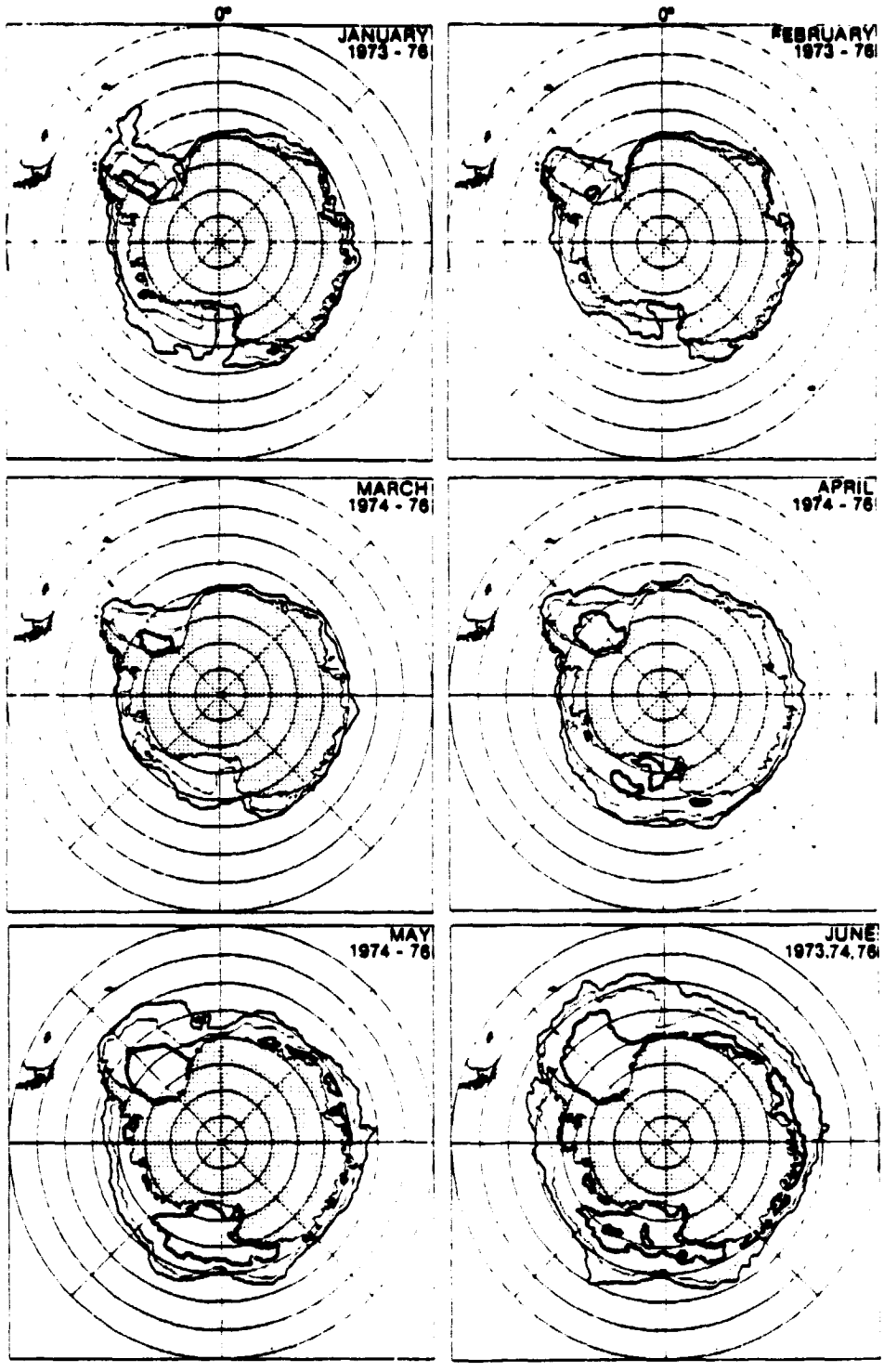

Figure 12. Multiyear monthly ice-concentrations contours for January through June 1973-1976.

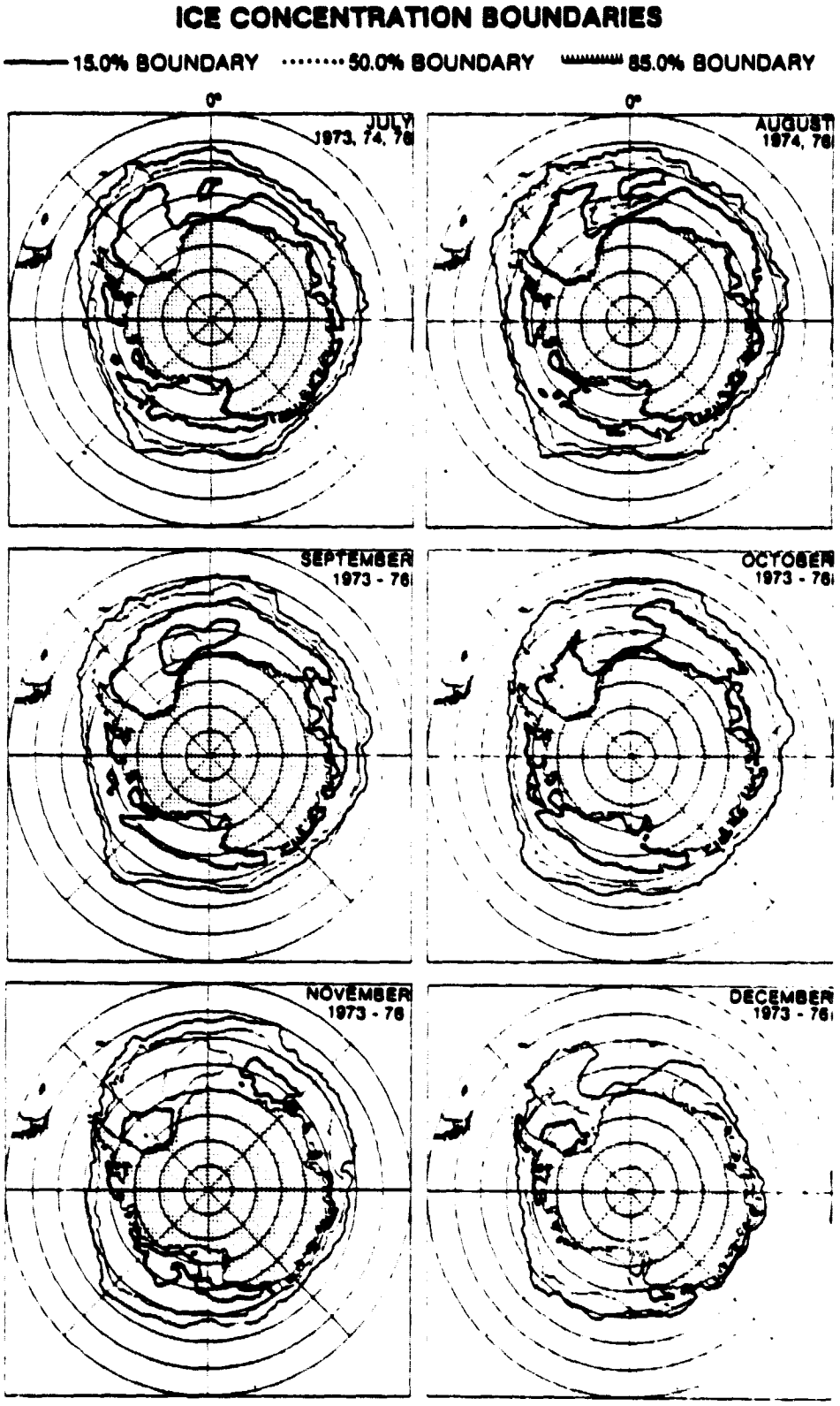

Figure 13. Multiyear monthly ice-concentrations contours for July through December 1973-1976.